

Solvation of UCl_6^{2-} Anionic Complex by MeBu_3N^+ , BuMe_2Im^+ , and BuMelm^+ CationsEmilie Bossé,[†] Christophe Den Auwer,[†] Claude Berthon,[†] Philippe Guilbaud,[†] Mikhail S. Grigoriev,[‡] Serguei Nikitenko,[§] Claire Le Naour,^{||} Céline Cannes,^{||} and Philippe Moisy^{*,†}

CEA Marcoule, DRCP/SCPS, BP 17171, 30207 Bagnols sur Cèze Cedex, France, A.N. Frumkin Institute of Physical Chemistry and Electrochemistry, RAS, Leninskii Prosp. 31, 119991 Moscow, Russia, CNAB, UMR 5084, CNRS, Université de Bordeaux I, BP 120 Le Haut Vigneau, 33175 Gradignan Cedex, France, and IPN, UMR 8608, CNRS, Université Paris-Sud, 91406 Orsay, France

Received December 21, 2007

The complexes $[\text{MeBu}_3\text{N}]_2[\text{UCl}_6]$ and $[\text{BuMe}_2\text{Im}]_2[\text{UCl}_6]$ were characterized in the solid state and in solution of $[\text{MeBu}_3\text{N}][\text{Tf}_2\text{N}]$, $[\text{BuMe}_2\text{Im}][\text{Tf}_2\text{N}]$, and $[\text{BuMelm}][\text{Tf}_2\text{N}]$ room-temperature ionic liquids using single-crystal XRD, EXAFS, electrochemistry, UV–visible absorption spectroscopy, and NMR. In the solid state and in solution, the existence of hydrogen bonding between the UCl_6^{2-} complex and the ionic liquid cations was revealed by these techniques. The MeBu_3N^+ cation interacts with UCl_6^{2-} via the protons on the α -carbon atoms of nitrogen. The protons of the imidazolium ring account for the interaction between the BuMe_2Im^+ cation and the UCl_6^{2-} anion. For the BuMelm^+ cation the major interaction was confirmed between the most acidic proton on C(2) and the chlorides of UCl_6^{2-} . The experimental results also show that the intensity of the interaction between the UCl_6^{2-} anion and the cation varies with the ionic liquid cation in the following order: $\text{MeBu}_3\text{N}^+ \approx \text{BuMe}_2\text{Im}^+ \ll \text{BuMelm}^+$.

1. Introduction

Room-temperature ionic liquids are remarkable solvents used in a large number of chemical processes including catalysis, organic synthesis, or electrochemistry.^{1–4} They are composed of an organic cation (alkylimidazolium, alkylpyridinium, tetraalkylammonium, etc.) and an inorganic anion (Cl^- , AlCl_4^- , PF_6^- , $(\text{CF}_3\text{SO}_2)_2\text{N}^-$, etc.). Their physical and chemical properties can be modified by selection of the appropriate cation/anion combination.³ Moreover, ionic liquids are relatively stable under radiation,^{5,6} providing a unique opportunity to investigate actinide chemistry by limiting the hydrolysis reactions of the tetravalent actinides.

Most published studies of actinides at the oxidation state +IV in ionic liquids concern their hexachloride complexes.^{7,8}

The spectroscopic and electrochemical behavior of these complexes has been studied in chloroaluminate ionic liquids,^{9–14} although they are extremely sensitive to air and water. Moreover, the Lewis acid–base properties depend on the molar fraction of constituents imparting additional complexing properties to these liquids via Cl^- , $\text{Al}_x\text{Cl}_y^{n-}$ anions capable of modifying the speciation of AnCl_6^{2-}

* To whom correspondence should be addressed. E-mail: philippe.moisy@cea.fr.

[†] CEA Marcoule.

[‡] A.N. Frumkin Institute of Physical Chemistry and Electrochemistry.

[§] Université de Bordeaux.

^{||} Université Paris-Sud.

(1) Earle, M. J.; Seddon, K. R. *Pure Appl. Chem.* **2000**, *72*, 1391–1398.

(2) Hagiwara, R.; Lee, J. S. *Electrochemistry* **2007**, *75*, 23–34.

(3) Wasserchied, P.; Welton, T. *Ionic Liquids in Synthesis*; Wiley-VCH: Weinheim, Germany, 2003.

(4) Welton, T. *Chem. Rev.* **1999**, *99*, 2071–2083.

(5) Allen, D.; Baston, G.; Bradley, A. E.; Gorman, T.; Haile, A.; Hamblett, I.; Hatter, J. E.; Healey, J. F.; Hodgdon, B.; Lewin, R.; Lovell, K. V.; Newton, B.; Pitner, W. R.; Rooney, D. W.; Sanders, D.; Seddon, K. R.; Sims, H. E.; Thied, R. C. *Green Chem.* **2002**, *4*, 152–158.

(6) (a) Berthon, L.; Nikitenko, S. I.; Bisel, I.; Berthon, C.; Faucon, M.; Saucerotte, B.; Zorz, N.; Moisy, P. *Dalton Trans.* **2006**, 2526–2534. (b) Bossé, E.; Berthon, L.; Zorz, N.; Berthon, C.; Bisel, I.; Legand, S.; Moisy, P. *Dalton Trans.* **2007**, 924–931.

(7) Cocalia, V. A.; Gutowski, K. E.; Rogers, R. D. *Coord. Chem. Rev.* **2006**, *250*, 755–764.

(8) Binnemans, K. *Chem. Rev.* **2007**, *107*, 2592–2614.

(9) Anderson, C. J.; Choppin, G. R.; Pruet, D. J.; Costa, D.; Smith, W. *Radiochim. Acta* **1999**, *84*, 31–36.

(10) Anderson, C. J.; Deakin, M. R.; Choppin, G. R.; D'Olieslager, W.; Heerman, L.; Pruet, D. J. *Inorg. Chem.* **1991**, *30*, 4013–4016.

(11) De Waele, R.; Heerman, L.; D'Olieslager, W. *J. Electroanal. Chem.* **1982**, *142*, 137–146.

(12) Hitchcock, P. B.; Mohammed, T. J.; Seddon, K. R.; Zora, J. A. *Inorg. Chim. Acta* **1986**, *113*, L25–L26.

(13) Hopkins, T. A.; Berg, R. W.; Costa, D.; Smith, W.; Dewey, H. J. *Inorg. Chem.* **2001**, *40*, 1820–1825.

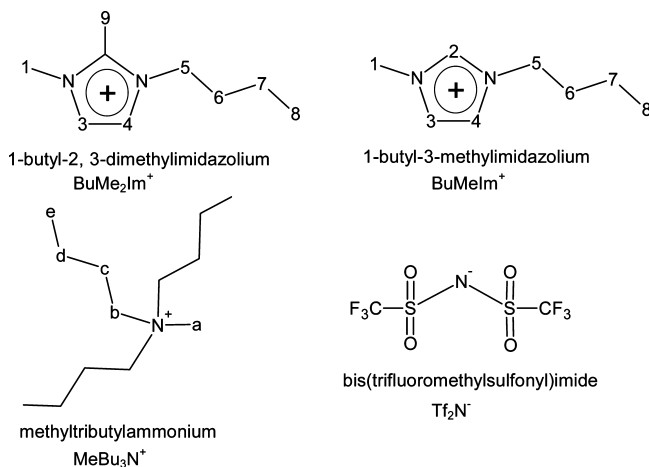
(14) Schoebsch, J. P.; Gilbert, B. P. *Inorg. Chem.* **1985**, *24*, 2105–2110.

anions. More recently, studies were carried out in room-temperature ionic liquids composed of the bis(trifluoromethylsulfonyl)imide anion noted Tf_2N^- .^{15,16} These recent UV/vis/NIR spectroscopy studies show that $AnCl_6^{2-}$ complexes, where An(IV) is U(IV), Np(IV), or Pu(IV), preserve the centrosymmetric octahedral environment of the actinide in these ionic liquids. Moreover, these complexes are stable with respect to hydrolysis. A more recent molecular dynamics study was reported by Schurhammer and Wipff¹⁷ on $U^{III}Cl_6^{3-}$, $U^{IV}Cl_6^{2-}$, and $U^{VI}Cl_6^-$ anions. These authors calculated the difference in solvation behavior in solution according to the charge of the anionic uranium complex and the cation in the ionic liquid. The calculations showed that the first solvation sphere of the UCl_6^{2-} anion is composed of 5.5 $BuMeIm^+$ cations for the ionic liquid $[BuMeIm][Tf_2N]$. For the ionic liquid $[MeBu_3N][Tf_2N]$, the calculations indicated that the first sphere is composed of four $MeBu_3N^+$ cations around the UCl_6^{2-} anion. The calculations also showed that the various ions interact through the hydrogen bond between the chlorides of the anionic complex and the protons of the imidazolium ring or the butyl chains of ammonium. Moreover, the calculations showed that the interaction is stronger with $[BuMeIm][Tf_2N]$ than with $[MeBu_3N][Tf_2N]$.¹⁷ The UCl_6^{2-} complexes were also studied in an acetonitrile medium in the presence of various alkylammonium salts.¹⁸ Ryan showed that the modification in the U(IV) absorption spectrum at wavelengths of 598, 657, and 672 nm is caused by hydrogen bonding between the UCl_6^{2-} anion and the alkylammonium salts.

A recent structural study of $[EtMeIm]_2[UCl_6]$ based on a statistical method developed by the authors revealed the presence of hydrogen bonds not only between the UCl_6^{2-} anion and the least acidic protons of the imidazolium ring but also with the first protons on the alkyl chains.¹⁹ However, another structural and spectroscopic study of $[BuMeIm]_2[UCl_6]$ as a solid or in solution in $[BuMeIm][Tf_2N]$ indicates the presence of a preferential hydrogen bond between the UCl_6^{2-} anion and the most acidic proton of the cation on the imidazolium ring.²⁰

In the light of these contradictory results, the present study based on spectroscopic and electrochemical measurements demonstrates the interaction by hydrogen bonding of the UCl_6^{2-} anionic complex with various ionic liquid cations. The ionic liquids selected for this study all included the Tf_2N^- anion. The corresponding cations were $MeBu_3N^+$, $BuMeIm^+$, and $BuMe_2Im^+$ (Scheme 1). The methyl group replacing the most acidic proton of the imidazolium ring has been used by various authors in particular to demonstrate

Scheme 1. Ionic Liquids Used



possible interactions between the cation and water.²¹ The properties of this ionic liquid, $[BuMe_2Im][Tf_2N]$, have recently been investigated and used by the authors for its chemical stability enhanced by the substitution of the most acidic proton.²² Using this ionic liquid enables the importance of the other two ring protons to be determined in the interaction between the $BuMeIm^+$ cation and the UCl_6^{2-} anion. Characterization of the solids $[MeBu_3N]_2[UCl_6]$ and $[BuMe_2Im]_2[UCl_6]$ is also reported.

2. Experimental Section

The ionic liquids $[MeBu_3N][Tf_2N]$ and $[BuMeIm][Tf_2N]$ purchased from Solvionic were used as received. The water concentrations of these ionic liquids, measured by coulometric Karl Fischer titration, were 0.04 and 0.03 M, respectively. The ionic liquids $[MeBu_3N]Cl$ and $[BuMe_2Im][Tf_2N]$ were prepared by a metathesis reaction from $[MeBu_3N]OH$ and HCl or $[BuMe_2Im]Cl$ and HTf_2N in an aqueous medium. Initial chemicals (Merck for ionic liquids and Aldrich for acids) were used in the synthesis without additional purification. The $[MeBu_3N]Cl$ was recovered by an organic phase CH_2Cl_2 . To remove chloride ions and proton impurities, the as-prepared RTIL $[BuMe_2Im][Tf_2N]$ was washed with deionized water (18 M Ω cm) to neutral pH. Organic impurities were removed from the RTIL with activated charcoal for 12 h, after which the mixture was passed through a column with small amounts of acidic alumina. The RTILs were dried overnight under reduced pressure (~5 mbar) at 80 °C. The water concentration in the dried RTIL was measured by coulometric Karl Fischer titration and found to be equal to 0.01 M. $[MeBu_3N]Cl$ was a white solid. $[BuMeIm]Cl$ was synthesized via quaternization of 1-methylimidazole by 1-chlorobutane and washed with ethyl acetate as recently described.³ It was dried overnight under reduced pressure (~5 mbar) at 80 °C. The ionic liquids $[BuMeIm][PF_6]$, $[BuMeIm][BF_4]$, and $[BuMeIm][Tf]$ (where Tf = trifluoromethanesulfonyl) were purchased from Merck. They were purified with activated charcoal for 12 h, after which the mixture was passed through a column with small amounts of acidic alumina. The RTILs were dried overnight under reduced pressure (~5 mbar) at 80 °C.

$[MeBu_3N]_2[UCl_6]$, $[BuMe_2Im]_2[UCl_6]$, and $[BuMeIm]_2[UCl_6]^{20}$ complexes were precipitated from U(IV) solution in concentrated

(15) Nikitenko, S. I.; Cannes, C.; Le Naour, C.; Moisy, P.; Trubert, D. *Inorg. Chem.* **2005**, *44*, 9497–9505.

(16) Nikitenko, S. I.; Moisy, P. *Inorg. Chem.* **2006**, *45*, 1235–1242.

(17) Schurhammer, R.; Wipff, G. *J. Phys. Chem. B* **2007**, *111*, 4659–4668.

(18) Ryan, J. L. *Inorg. Chem.* **1964**, *3*, 211–214.

(19) Deetlefs, M.; Hussey, C. L.; Mohammed, T. J.; Seddon, K. R.; Van den Berg, J.-A.; Zora, J. A. *Dalton Trans.* **2006**, 2334–2341.

(20) Nikitenko, S. I.; Hennig, C.; Grigoriev, M. S.; Le Naour, C.; Cannes, C.; Trubert, D.; Bossé, E.; Berthon, C.; Moisy, P. *Polyhedron* **2007**, *26*, 3136–3142.

(21) Cammarata, L.; Kazarian, S. G.; Salter, P. A.; Welton, T. *Phys. Chem. Chem. Phys.* **2001**, *3*, 5192–5200.

(22) Bazito, F. F. C.; Kawano, Y.; Torresi, R. M. *Electrochim. Acta* **2007**, *52*, 6427–6437.

HCl in the presence of a slight excess of [MeBu₃N]Cl, [BuMe₂Im]Cl, and [BuMeIm]Cl, respectively. To obtain single crystals of [MeBu₃N]₂[UCl₆] or [BuMeIm]₂[UCl₆], the powder was recrystallized from a MeOH/MeCN (50/50) mixture under reduced pressure.²⁰

The X-ray structural experiments were carried out on a Nonius KappaCCD diffractometer (Mo K α radiation, graphite monochromator). To prevent the crystal, which was unstable in air, from decomposing and to reduce thermal motion, the experiment was carried out at low temperature. The crystal was mounted in a glass capillary with Paratone-N grease. The distance from the crystal to the area-sensitive detector was 30 mm; half of the reciprocal space was measured up to a maximum diffraction angle of 27.5°. The data were processed with HKL.²³ The experimental intensities for crystals containing heavy atoms were corrected for absorption using the MULABS procedure in the PLATON suite.²⁴ The structure was solved with SHELXS97 and refined with SHELXL97.²⁵ The H atoms of CH₂ and CH₃ groups were refined in idealized positions with displacement parameters equal to 1.2 (CH₂) or 1.5 (CH₃) times those of the attached carbon atoms.

EXAFS data of [MeBu₃N]₂[UCl₆] dissolved in [MeBu₃N][Tf₂N] (0.01 mol L⁻¹) and [BuMe₂Im]₂[UCl₆] dissolved in [BuMe₂Im][Tf₂N] (0.01 mol L⁻¹) were recorded at the Stanford Synchrotron Radiation Laboratory (SSRL) on the 11-2 beam line and at the European Synchrotron Research Facility (ESRF) on the BM20 ROBL beam line. SSRL (3.0 GeV at 100 mA): fluorescence mode at room temperature, with a Si(220) nitrogen-cooled monochromator in a channel-cut mode, Rh mirror for harmonic rejection. ESRF (6.0 GeV at 200 mA): fluorescence mode at room temperature, with a Si(111) water-cooled monochromator in a channel-cut mode, Pt mirror for harmonic rejection. Energy calibration was carried out with a Y foil (17052 eV at the absorption maximum), and E₀ value (17175.4 eV) was determined by the first inflection point of the absorption maximum. All data processing (AUTOBK normalization) was done with the Athena code.²⁶ Data fitting was carried out with the Artemis code²⁶ in *R*-space after Fourier transformation in *k*³ between 3 and 12 Å⁻¹. Phases and amplitudes were calculated with the Feff8.2 code from a UCl₆ octahedron in a vacuum obtained from the crystal structure of [BuMeIm]₂[UCl₆].²⁰

¹H NMR spectra were measured with a Varian-INOVA 400 NMR spectrometer in anhydrous CH₂Cl₂ solutions. The CH₂Cl₂ diluent was presaturated for convenience to avoid signal overload and overlay off the RTIL's peaks. The ¹H chemical shifts were externally referenced to benzene-*d*₆ at 7.15 ppm.

UV-vis spectra were collected with a Shimadzu UV-3101 PC spectrophotometer using 1 cm quartz cells sealed airtight by Teflon stoppers. The UV-vis spectra of solids were obtained in pellets with 5 mg of product and 45 mg of NaCl under a pressure of approximately 8000 psi.

A Golden Gate ATR-IR system using a diamond as the ATR crystal was used to obtain IR spectra, which were measured on a Bruker Equinox-55 FTIR spectrometer with a DTGS detector and a resolution of 0.5 cm⁻¹.

The voltammetric study was carried out with an Autolab PGSTAT 30 device. A commercial thermostated three-electrode Pyrex electrochemical cell (*V* = 4 mL) was used with a 3 mm Radiometer glassy carbon (GC) disk working electrode and Pt counterelectrode. The reference electrode was prepared by immer-

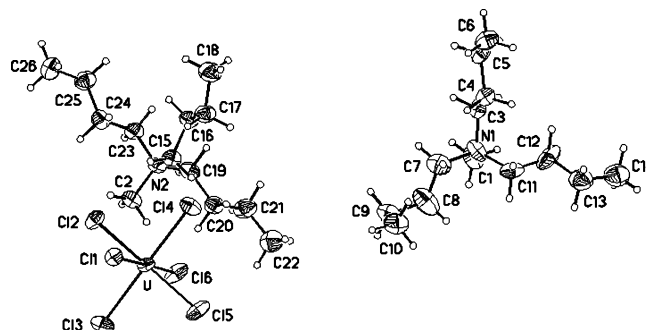


Figure 1. View of [MeBu₃N]₂[UCl₆], showing the atom-labeling scheme. Displacement ellipsoids are drawn at the 50% probability level, and H atoms are represented by circles of arbitrary size.

Table 1. Crystallographic Data for [MeBu₃N]₂[UCl₆]

chemical formula	C ₂₆ H ₃₀ Cl ₆ N ₂ U
space group	P $\bar{1}$
<i>a</i> (Å)	9.9717(2)
<i>b</i> (Å)	10.7861(2)
<i>c</i> (Å)	17.8015(5)
α (deg)	74.3261(14)
β (deg)	82.4928(13)
γ (deg)	89.6077(15)
<i>V</i> (Å ³)	1826.84(7)
ρ_{calcd} (g cm ⁻³)	1.548
<i>Z</i>	2
<i>R</i> 1 (<i>I</i> > 2 σ (<i>I</i>))	0.0409
<i>wR</i> 2 (all data)	0.0998

sion of the Ag wire in a 0.01 M solution of [Ag][CF₃SO₃] in [BuMeIm][Tf₂N]. The reference solution was placed in a glass liquid junction protection tube with a fine porosity frit (from Radiometer). All potentials are reported with respect to this reference. The working electrode was polished on emery paper with different grain sizes. The cell was deaerated with argon (O₂ < 0.1 ppm and H₂O < 0.5 ppm) for 30 min before the measurements. Argon was also sparged into the cell during the electrochemical data acquisition. The electrochemical measurements were performed at 25 ± 1 °C, with the temperature controlled by a Polystat 5 water thermostat. All cyclic voltammograms were compensated for ohmic drop by the positive feedback process of the Autolab PGSTAT 30 software. The redox potential of the ferrocenium/ferrocene couple (Fc⁺/Fc) measured under these conditions by cyclic voltammetry with ohmic drop compensation is -0.36 V vs Ag/Ag(I) in [BuMeIm][Tf₂N] and -0.33 V vs Ag/Ag(I) in [MeBu₃N][Tf₂N]. The *E*_{1/2} value corresponds to the voltammetric half-wave potentials and was measured from cyclic staircase voltammograms (*E*_{pa} + *E*_{pc})/2.

All molecular structures were fully optimized using Gaussian 03 at the Hartree-Fock level using the 6-31+G** basis set. Electrostatic potential calculations were performed at the same level using the Merz-Kollman method. Surfaces were represented using Molekel 5.2 mapping electrostatic potential at the accessible solvent surface with a solvent probe radius of 0.5 Å.

3. Results

3.1. Solid-State Characterization. The structure of the [MeBu₃N]₂[UCl₆] complex is shown in Figure 1, and crystal data are given in Table 1. The UCl₆²⁻ anion in [MeBu₃N]₂[UCl₆] exhibits a slightly distorted octahedral structure. Table 2 indicates that the U-Cl distances in UCl₆²⁻ anion range between 2.6026(13) and 2.6413(12) Å. The average value of 2.624(5) Å is in a good agreement with the average value of 2.616(4) Å for seven compounds with UCl₆²⁻ anions from

(23) Otwinowski, Z.; Minor, W. *Macromolecular Crystallography Part A: Methods in Enzymology*. Carter, C. W., Jr., Sweet, R. M., Eds.; Academic Press: New York, 1997; Vol. 276, pp 307-326.

(24) Spek, A. L. *J. Appl. Cryst.* **2003**, *36*, 7-13.

(25) Sheldrick, G. M. *SHELXL97* and *SHELXS97*; University of Göttingen: Göttingen, Germany, 1997.

(26) Ravel, B.; Newville, M. *J. Synchrotron Radiat.* **2005**, *12*, 537.

Table 2. U–Cl Bond Lengths in $[\text{MeBu}_3\text{N}]_2[\text{UCl}_6]$

bond	distance (Å)
U–Cl1	2.6413(12)
U–Cl2	2.6248(11)
U–Cl3	2.6220(15)
U–Cl4	2.6259(15)
U–Cl5	2.6256(12)
U–Cl6	2.6026(13)

the Cambridge Structural Database and especially with the structure of $[\text{BuMeIm}]_2[\text{UCl}_6]$ recently determined in our laboratory.²⁰

The two MeBu_3N^+ cations shown in Figure 1 differ by their conformations and contacts with UCl_6^{2-} anions. For the first MeBu_3N^+ conformation cation, the shortest $\text{U}\cdots\text{N}$ distances are 5.978(5) and 6.057(5) Å in the $[\text{MeBu}_3\text{N}]_2[\text{UCl}_6]$ compound. For the second MeBu_3N^+ conformation, the shortest $\text{U}\cdots\text{N}$ distances are 5.425(4) and 5.605(4) Å. This structure also comprises several short $\text{H}\cdots\text{Cl}$ contacts that can be attributed to H-bonds. More precisely, there are six contacts with $\text{H}\cdots\text{Cl}$ distances of less than 2.95 Å, the shortest of which is 2.68 Å. Three H atoms are from methyl groups (protons a on the Scheme 1) and three other protons from the first CH_2 (near N) of butyl groups (protons b on the Scheme 1). However, the contact between MeBu_3N^+ and UCl_6^{2-} is larger than the contact between BuMeIm^+ and UCl_6^{2-} (2.57 Å for the shortest contact),²⁰ so the interaction between the proton and the chloride is more intense with the BuMeIm^+ cation.

The IR spectra of the solids $[\text{MeBu}_3\text{N}]_2[\text{UCl}_6]$, $[\text{BuMeIm}]_2[\text{UCl}_6]$, and $[\text{BuMe}_2\text{Im}]_2[\text{UCl}_6]$ obtained in the 4000–600 cm^{-1} region are provided in the Supporting Information. The 1600–600 cm^{-1} region shows deformation of the alkyl chains of the MeBu_3N^+ cation or internal vibrations of the imidazolium ring. The most interesting region is the elongation of the alkyl chains and ring between 3200 and 2600 cm^{-1} . Figure 2 shows the IR spectra of the solids $[\text{MeBu}_3\text{N}]_2[\text{UCl}_6]$, $[\text{BuMeIm}]_2[\text{UCl}_6]$, and $[\text{BuMe}_2\text{Im}]_2[\text{UCl}_6]$. None of these complexes exhibits a broadband above 3200 cm^{-1} , indicating that the uranium compounds are not hydrated. The spectra of each complex were compared in pairs with that of the corresponding chloride ionic liquid, that is, $[\text{MeBu}_3\text{N}]\text{Cl}$, $[\text{BuMeIm}]\text{Cl}$, and $[\text{BuMe}_2\text{Im}]\text{Cl}$.

The spectra of $[\text{MeBu}_3\text{N}]_2[\text{UCl}_6]$ and $[\text{MeBu}_3\text{N}]\text{Cl}$ (Figure 2a) are similar throughout the wavenumber range investigated. The band between 3550 and 3000 cm^{-1} correspond to the presence of the small amount of water in the $[\text{MeBu}_3\text{N}]\text{Cl}$ solid. So, the only difference between the two compounds is the band shift for the $\text{N}-\text{CH}_3$ bond: 3034 cm^{-1} for $[\text{MeBu}_3\text{N}]_2[\text{UCl}_6]$ and 3006 cm^{-1} for $[\text{MeBu}_3\text{N}]\text{Cl}$.

The shift toward lower wavenumbers indicates the presence of an interaction between the methyl group of the MeBu_3N^+ cation and the anion. The intensity of the interaction between the MeBu_3N^+ cation and the anions can be ranked in the following order: $\text{UCl}_6^{2-} < \text{Cl}^-$.

Several differences are highlighted by comparing the IR spectra of $[\text{BuMeIm}]_2[\text{UCl}_6]$ and $[\text{BuMeIm}]\text{Cl}$ (Figure 2b):

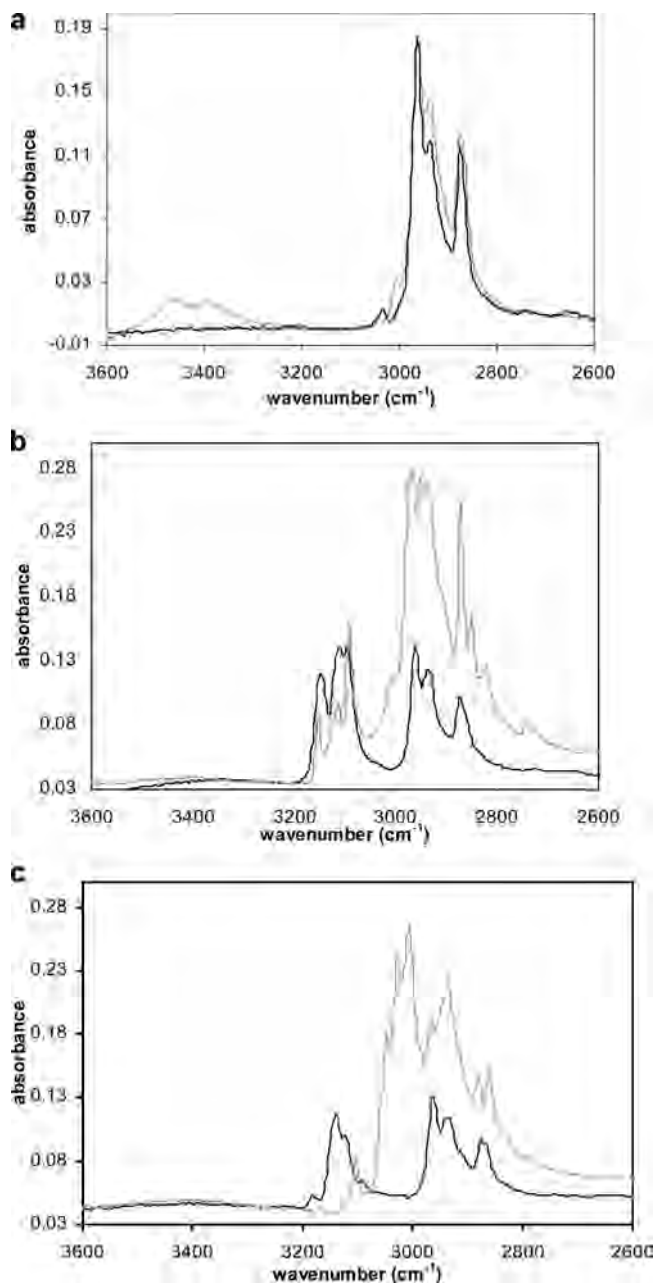
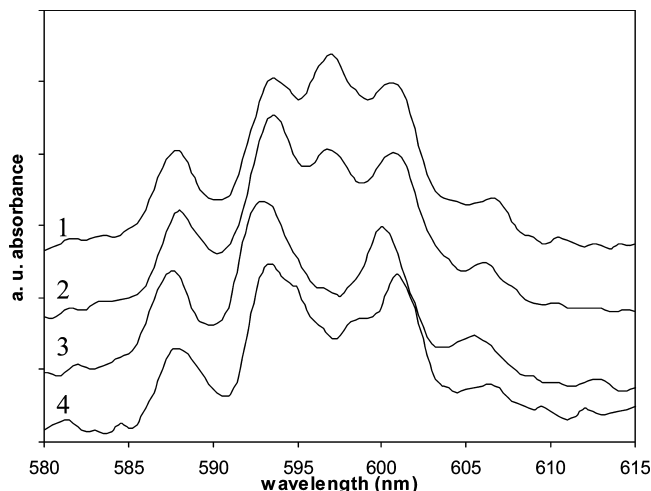


Figure 2. (a) IR spectra of $[\text{MeBu}_3\text{N}]_2[\text{UCl}_6]$ (black) and $[\text{MeBu}_3\text{N}]\text{Cl}$ (gray). (b) IR spectra of $[\text{BuMeIm}]_2[\text{UCl}_6]$ (black) and $[\text{BuMeIm}]\text{Cl}$ (gray). (c) IR spectra of $[\text{BuMe}_2\text{Im}]_2[\text{UCl}_6]$ (black) and $[\text{BuMe}_2\text{Im}]\text{Cl}$ (gray).

- (i) Higher intensity of the skeletal bands caused by the inductive effects of the Cl^- anion on the imidazolium ring.
 - (ii) Splitting of the bands for the alkyl chains (3000–2900 cm^{-1}) with the Cl^- anion because of the interaction between the Cl^- anion and the alkyl chains. The interaction with protons of the butyl chain or methyl group was not observed for the UCl_6^{2-} anion and can be considered negligible.
- (a) A new vibration band for the imidazolium ring with the Cl^- and UCl_6^{2-} anion around 3090 cm^{-1} (Table 3). Tait and Osteryoung,²⁷ as well as Hitchcock et al.,²⁸ had already observed this phenomenon and attributed it to a hydrogen bond.

Table 3. Wavenumber (cm^{-1}) for Imidazolium Ring Vibration Obtained for Different Anions Bonded to Cation BuMeIm^+ ^a

anion	cycle HC(3)–C(4)H	cycle N–C(2)–N	aromatic C(2)–H···X
PF_6^-	3172	3125	
BF_4^-	3162	3122	
Tf_2N^-	3158	3121	
Tf^-	3154	3114	
Cl^-	3153	3113	3091
UCl_6^{2-}	3150	3111	3095

^a Assignment based on the data in Scheme 1.**Figure 3.** UV–vis spectra of solid compounds (1) $[\text{BuMeIm}]_2[\text{UCl}_6]$, (2) $[\text{MeBu}_3\text{N}]_2[\text{UCl}_6]$, (3) $[\text{BuMe}_2\text{Im}]_2[\text{UCl}_6]$, and (4) $\text{Cs}_2[\text{UCl}_6]$ on pellets containing 5 mg of product and 45 mg of dry NaCl.

These modifications indicate the presence of a hydrogen bond interaction between the BuMeIm^+ cation and the Cl^- or UCl_6^{2-} anion. Moreover, the UCl_6^{2-} anion induces a slight redshift of the imidazolium ring vibration bands. This shift toward lower wavenumbers was used by Suarez et al.²⁹ to assess the intensity of the hydrogen bond in $[\text{BuMeIm}][\text{BF}_4]$ and $[\text{BuMeIm}][\text{PF}_6]$ ionic liquids. The interaction between the aromatic proton of the BuMeIm^+ cation and the UCl_6^{2-} anion is thus stronger than with the Cl^- anion ($\text{Cl}^- < \text{UCl}_6^{2-}$).

The IR spectra of $[\text{BuMe}_2\text{Im}]_2[\text{UCl}_6]$ and $[\text{BuMe}_2\text{Im}]\text{Cl}$ also differ (Figure 2c). The characteristic bands of the alkyl and aromatic chains were split for $[\text{BuMe}_2\text{Im}]\text{Cl}$. They also exhibited higher intensity and were shifted by about 120 cm^{-1} toward lower wavenumbers compared with the $[\text{BuMe}_2\text{Im}]_2[\text{UCl}_6]$ spectrum.

The spectrum for $[\text{BuMe}_2\text{Im}]\text{Cl}$ is consistent with the data reported by Kölle et al.³⁰ The interaction between the BuMe_2Im^+ cation and the Cl^- anion is thus stronger than with the UCl_6^{2-} anion. The intensity of the interaction between the anions and the BuMe_2Im^+ cation increases in the following order: $\text{UCl}_6^{2-} \ll \text{Cl}^-$.

The absorption spectra of the solids $[\text{BuMe}_2\text{Im}]_2[\text{UCl}_6]$ and $[\text{MeBu}_3\text{N}]_2[\text{UCl}_6]$ diluted in a solid NaCl matrix are shown in Figure S4. Figure 3 shows these spectra between 580 and 615 nm.

Table 4. ^1H NMR Spectral Data for $[\text{MeBu}_3\text{N}]_2[\text{UCl}_6]$ dissolved in a Minimum of CH_2Cl_2

δ (ppm)	multiplicity	integration	assignment ^a
2.953	triplet	6	H(a)
2.536	singlet	3	H(b)
1.774	multiplet	11.5	H(c)
1.774	multiplet	11.5	H(d)
1.408	triplet	7.7	H(e)

^a See Scheme 1.**Table 5.** ^1H NMR Spectral Data for $[\text{BuMe}_2\text{Im}]_2[\text{UCl}_6]$ dissolved in a Minimum of CH_2Cl_2

δ (ppm)	multiplicity	integration	assignment ^a
7.02	doublet	1	H(3)
6.96	doublet	1	H(4)
3.92	triplet	2	H(5)
3.47	singlet	3	H(1)
2.21	singlet	3	H(9)
1.79	multiplet	2	H(6)
1.43	multiplet	2	H(7)
1.03	triplet	3	H(8)

^a See Scheme 1.

The spectra of the two solid compounds $[\text{BuMeIm}]_2[\text{UCl}_6]$ and $\text{Cs}_2[\text{UCl}_6]$ were also recorded under the same conditions and are shown in Figure 3. Only the spectral region between 580 and 615 nm exhibits an actual difference between cations MeBu_3N^+ , BuMeIm^+ , BuMe_2Im^+ , and Cs^+ : an additional peak is observed at 597 nm. This peak was absent for solid $\text{Cs}_2[\text{UCl}_6]$ and $[\text{BuMe}_2\text{Im}]_2[\text{UCl}_6]$ and had a much higher intensity for solid $[\text{BuMeIm}]_2[\text{UCl}_6]$ than for solid $[\text{MeBu}_3\text{N}]_2[\text{UCl}_6]$. The ratio of the absorbance at 597 and 593.5 nm was determined to be 0.49, 0.5, 0.82, and 1.15, respectively, for cations Cs^+ , BuMe_2Im^+ , MeBu_3N^+ , and BuMeIm^+ . In agreement with the findings reported by Ryan¹⁸ in acetonitrile, the difference in the UCl_6^{2-} spectrum for complexes with different cations indicates an interaction in the solid between the UCl_6^{2-} anion and the ionic liquid cation. The intensity of this interaction varies in the following order: $\text{Cs}^+ \approx \text{BuMe}_2\text{Im}^+ < \text{MeBu}_3\text{N}^+ < \text{BuMeIm}^+$.

The ^1H NMR spectra of solutes $[\text{MeBu}_3\text{N}]_2[\text{UCl}_6]$ and $[\text{BuMe}_2\text{Im}]_2[\text{UCl}_6]$ were obtained by dissolution of these solid compounds in a small volume of dichloromethane to avoid possible interactions between the ions.³¹ The ^1H NMR spectra of $[\text{MeBu}_3\text{N}]\text{Cl}$ and $[\text{BuMe}_2\text{Im}]\text{Cl}$ were also obtained under the same conditions.

The proton signal assignments for the MeBu_3N^+ cation are indicated together with the chemical shifts in Table 4. The similar chemical shift for protons b and c (Scheme 1) of solute $[\text{MeBu}_3\text{N}]_2[\text{UCl}_6]$ appears to be caused only by the conformation of the alkyl chains. Table 5 lists the data for the BuMe_2Im^+ cation. Note that uranium(IV) paramagnetism results in an isotropic shift to lower fields and broadening of the peaks for uranium complexes.

Figure 4 shows the chemical shifts for the protons of $[\text{BuMe}_2\text{Im}]_2[\text{UCl}_6]$ and $[\text{BuMeIm}]_2[\text{UCl}_6]$ ²⁰ versus the proton chemical shifts of $[\text{BuMe}_2\text{Im}]\text{Cl}$ and $[\text{BuMeIm}]\text{Cl}$, respectively. The linear correlation between the proton chemical shifts for $[\text{BuMe}_2\text{Im}]_2[\text{UCl}_6]$ and $[\text{BuMe}_2\text{Im}]\text{Cl}$ shows that

(27) Tait, S.; Osteryoung, R. A. *Inorg. Chem.* **1984**, *23*, 4352–4360.(28) Hitchcock, P. B.; Seddon, K. R.; Welton, T. *Dalton Trans.* **1993**, 2639–2643.(29) Suarez, P. A. Z.; Einloft, S.; Dullius, J. E. L.; de Souza, R. F.; Dupont, J. J. *Chim. Phys.* **1998**, *95*, 1626–1639.(30) Kölle, P.; Dronskowski, R. *Inorg. Chem.* **2004**, *43*, 2803–2809.(31) Li, W.; Zhang, Z.; Han, B.; Hu, S.; Xie, Y.; Yang, G. *J. Phys. Chem. B* **2007**, *111*, 6452–6456.

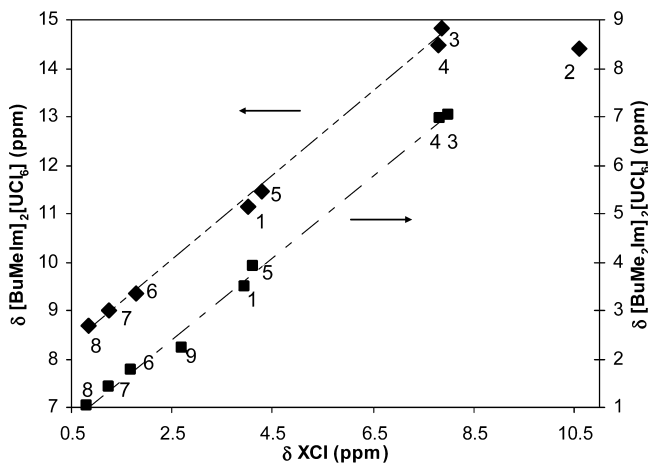


Figure 4. Relation between ^1H NMR chemical shifts of XCl and $[\text{X}]_2[\text{UCl}_6]$ where $\text{X} = \text{BuMeIm}^+$ (\blacklozenge), $^{20}\text{BuMe}_2\text{Im}^+$ (\blacksquare) in CH_2Cl_2 . The assignment is based on the data in Scheme 1.

Table 6. ^1H NMR Chemical Shift of H(2) for BuMeIm^+ Cation^a for Various Anions

anion	δ of H(2) (ppm)
PF_6^-	8.27
BF_4^-	8.53
Tf_2N^-	8.57
Tf^-	8.9
Cl^-	10.61
UCl_6^{2-}	14.41

^a See Scheme 1.

Table 7. U–Cl Distances Determined by EXAFS for Liquid Complexes $[\text{MeBu}_3\text{N}]_2[\text{UCl}_6]$ in $[\text{MeBu}_3\text{N}][\text{Tf}_2\text{N}]$ (0.01 M) and $[\text{BuMe}_2\text{Im}]_2[\text{UCl}_6]$ in $[\text{BuMe}_2\text{Im}][\text{Tf}_2\text{N}]$ (0.01 M) and Comparison with Literature Data of $[\text{BuMeIm}]_2[\text{UCl}_6]$ in $[\text{BuMeIm}][\text{Tf}_2\text{N}]$ and Solid $[\text{BuMeIm}]_2[\text{UCl}_6]$

	MeBu_3N^+	BuMe_2Im^+	BuMeIm^{+20}	$\text{BuMeIm}^+_{(\text{solid})}^{20}$
$d_{\text{U-Cl}}$	2.66(1) Å	2.64(1) Å	2.632 Å	2.619 Å
e_0	5.23 eV	4.00 eV		
S_0^2	0.9	0.9		
σ^2	0.0057 Å ²	0.0057 Å ²		

none of the protons of the BuMe_2Im^+ cation interacts specifically with the UCl_6^{2-} anion, contrary to what has already been demonstrated for the most acidic proton (on carbon C(2)) of the imidazolium ring of the BuMeIm^+ cation.²⁰ The study performed with the MeBu_3N^+ cation also showed a linear correlation between the proton chemical shifts of $[\text{MeBu}_3\text{N}]_2[\text{UCl}_6]$ and $[\text{MeBu}_3\text{N}]\text{Cl}$ (Figure S5), and the MeBu_3N^+ cation does not exhibit any specific interaction with the UCl_6^{2-} anion.

Table 6 indicates the chemical shifts of proton H(2) on the BuMeIm^+ cation for various anions. The proton unshielding indicates an interaction between the cation and anion.²⁰ The strength of this interaction depends on the anion in the following order: $\text{PF}_6^- < \text{BF}_4^- < \text{Tf}_2\text{N}^- < \text{Tf}^- < \text{Cl}^- < \text{UCl}_6^{2-}$.

3.2. Study in Solution. EXAFS measurements were recorded to determine the U(IV) coordination in solution of both complexes $[\text{MeBu}_3\text{N}]_2[\text{UCl}_6]$ dissolved in $[\text{MeBu}_3\text{N}][\text{Tf}_2\text{N}]$ and $[\text{BuMe}_2\text{Im}]_2[\text{UCl}_6]$ dissolved in $[\text{BuMe}_2\text{Im}][\text{Tf}_2\text{N}]$. Data for both liquid and solid $[\text{BuMeIm}]_2[\text{UCl}_6]$ are taken from ref 20. All the EXAFS spectra exhibit a monotonous wave that is characteristic of a single shell of neighbors at a single distance (Figure S6). This is consistent with the

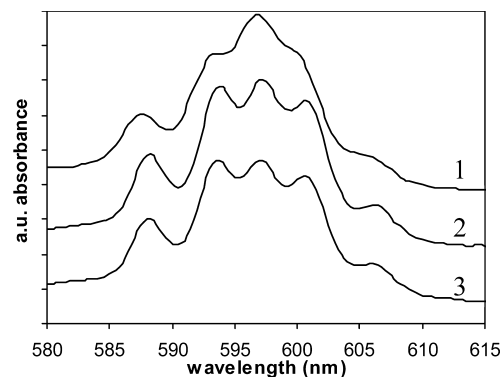


Figure 5. UV–vis spectra between 580 and 615 nm of (1) $[\text{BuMeIm}]_2[\text{UCl}_6]$, (2) $[\text{BuMe}_2\text{Im}]_2[\text{UCl}_6]$, and (3) $[\text{MeBu}_3\text{N}]_2[\text{UCl}_6]$ dissolved (7.74×10^{-3} M), respectively, in $[\text{BuMeIm}][\text{Tf}_2\text{N}]$, $[\text{BuMe}_2\text{Im}][\text{Tf}_2\text{N}]$, and $[\text{MeBu}_3\text{N}][\text{Tf}_2\text{N}]$.

Table 8. Molar Extinction Coefficients for Selected Wavelengths for $[\text{MeBu}_3\text{N}]_2[\text{UCl}_6]$, $[\text{BuMe}_2\text{Im}]_2[\text{UCl}_6]$ and $[\text{BuMeIm}]_2[\text{UCl}_6]$ dissolved Respectively in $[\text{MeBu}_3\text{N}][\text{Tf}_2\text{N}]$, $[\text{BuMe}_2\text{Im}][\text{Tf}_2\text{N}]$ and $[\text{BuMeIm}][\text{Tf}_2\text{N}]$

ϵ ($\text{L} \cdot \text{mol}^{-1} \cdot \text{cm}^{-1}$)	$[\text{MeBu}_3\text{N}]_2[\text{UCl}_6]$	$[\text{BuMe}_2\text{Im}]_2[\text{UCl}_6]$	$[\text{BuMeIm}]_2[\text{UCl}_6]$
452 nm	5.5 ± 0.3	6.4 ± 0.3	5.4 ± 0.3
597 nm	5.3 ± 0.3	6.2 ± 0.3	6.5 ± 0.3
635 nm	2.5 ± 0.1	3.1 ± 0.2	3.1 ± 0.2
777 nm	1.79 ± 0.09	1.49 ± 0.07	2.3 ± 0.1

presence in all the samples of a UCl_6^{2-} octahedron (coordination number fixed in the fit).

Table 7 indicates the U–Cl distances obtained from the best-fit parameters. For the MeBu_3N^+ cation, the first coordination sphere of uranium is composed of six chlorides at a mean distance of 2.66(1) Å. This distance is slightly longer than that determined by single-crystal XRD in the solid compound (2.62 Å). For the BuMe_2Im^+ cation, the mean U–Cl distance is 2.64(1) Å. The shortest U–Cl bond corresponds to $[\text{BuMeIm}]_2[\text{UCl}_6]$ with U–Cl distances of 2.63(1) Å. Although the discrepancy between all the distances is of the order of the uncertainty (between 0.01 and 0.02 Å), it appears that the mean U–Cl distance slightly increases according to the cation in the following order: $\text{BuMeIm}^+ < \text{BuMe}_2\text{Im}^+ < \text{MeBu}_3\text{N}^+$. Furthermore, the Debye–Waller factor corresponding to the three solutions are comparable (around 0.0050 Å²), indicating in a first approximation that the ordering of the uranium coordination sphere is comparable in all the solutions. It also compares very well with the solid state sample of ref 20 (0.0045 Å²), suggesting that the structural disorder in solution is comparable to that in the crystal structure.

Figure 5 shows the absorption spectra between 580 and 615 nm of UCl_6^{2-} complexes dissolved in ionic liquids $[\text{MeBu}_3\text{N}][\text{Tf}_2\text{N}]$, $[\text{BuMe}_2\text{Im}][\text{Tf}_2\text{N}]$, and $[\text{BuMeIm}][\text{Tf}_2\text{N}]$. Depending on the ionic liquid cation, the peak at 597 nm does not have the same intensity, and the absorbance ratio at 597 and 593.5 nm also differs according to the cation: the ratios are 1, 1.03, and 1.31, respectively, for cations MeBu_3N^+ , BuMe_2Im^+ , and BuMeIm^+ . The intensity of the 656 and 671 nm peaks also increases, although the resolution in this portion of the spectrum is not sufficient to allow proper interpretation (Figure S7). The major increase in the 597 nm peak and the spectral modification at 660 nm indicate a

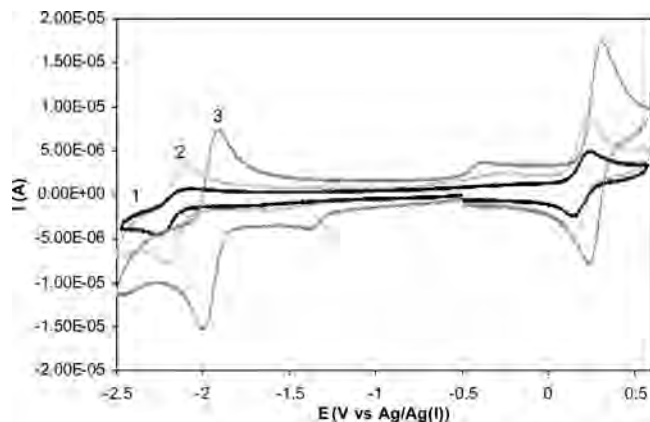


Figure 6. Cyclic voltammograms of $[\text{MeBu}_3\text{N}]_2[\text{UCl}_6]$ dissolved (0.01 M) in (1) $[\text{MeBu}_3\text{N}][\text{Tf}_2\text{N}]$, (2) $[\text{BuMe}_2\text{Im}][\text{Tf}_2\text{N}]$, and (3) $[\text{BuMeIm}][\text{Tf}_2\text{N}]$ with a GC electrode (area 0.07 cm^2) at $25 \text{ }^\circ\text{C}$. $\nu = 100 \text{ mV s}^{-1}$.

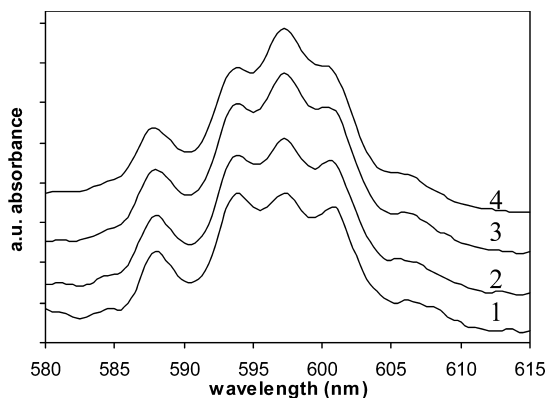


Figure 7. Absorption spectra of UCl_6^{2-} between 580 and 615 nm in a solution of $[\text{MeBu}_3\text{N}]_2[\text{UCl}_6]$ dissolved ($3 \times 10^{-3} \text{ M}$) in $[\text{MeBu}_3\text{N}][\text{Tf}_2\text{N}]$ versus molar fraction of $[\text{BuMeIm}][\text{Tf}_2\text{N}]$ (1: none, 2: 0.23, 3: 0.35, 4: 0.61).

hydrogen bonding¹⁸ between the UCl_6^{2-} anion and the BuMeIm^+ cation. The octahedral complex around the U^{4+} ion is deformed sufficiently by the hydrogen bond to allow symmetry-forbidden electronic transitions. Moreover, the 597 nm peak remains associated with two $5f \rightarrow 5f$ vibronic transitions at 593 and 601 nm.

The molar extinction coefficients of the UCl_6^{2-} complex for each ionic liquid cation at different wavelengths are indicated in Table 8. The coefficients are comparable for all the cations, although the molar extinction coefficient at 597 nm is slightly higher for BuMeIm^+ than for the other cations. The coefficient at 452 nm is also significantly higher for BuMe_2Im^+ than for the other cations.

Figure 6 shows the cyclic voltammograms of UCl_6^{2-} complex dissolved in ionic liquids $[\text{MeBu}_3\text{N}][\text{Tf}_2\text{N}]$, $[\text{BuMeIm}][\text{Tf}_2\text{N}]$, and $[\text{BuMe}_2\text{Im}][\text{Tf}_2\text{N}]$ between -2.5 and 0.6 V vs $\text{Ag}/\text{Ag}(\text{I})$. The UCl_6^{2-} voltammogram reveals several electrochemical systems previously identified by Nikitenko et al.¹⁵

A preliminary analysis of these results indicates that the half-wave potentials of each system have different values depending on the ionic liquid cation. The potential of the $\text{U}(\text{IV})/\text{U}(\text{III})$ couple is -2.2 , -2.13 , and -1.95 V vs $\text{Ag}/\text{Ag}(\text{I})$ in ionic liquids $[\text{MeBu}_3\text{N}][\text{Tf}_2\text{N}]$, $[\text{BuMe}_2\text{Im}][\text{Tf}_2\text{N}]$,

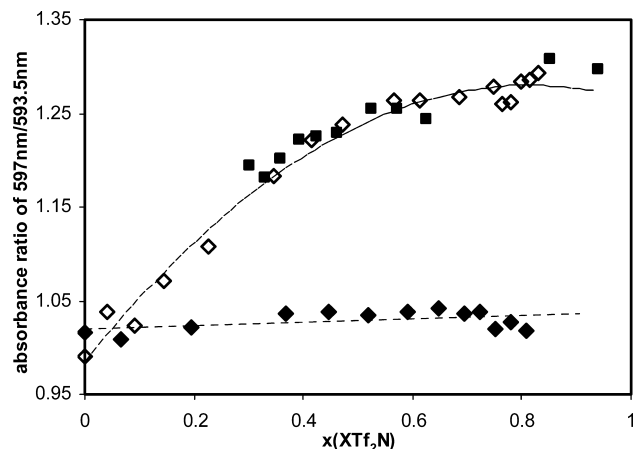


Figure 8. Absorbance ratio at wavelengths 597 and 593.5 nm of a solution of $[\text{MeBu}_3\text{N}]_2[\text{UCl}_6]$ dissolved ($3 \times 10^{-3} \text{ M}$) in $[\text{MeBu}_3\text{N}][\text{NTf}_2\text{N}]$ with addition of (\diamond) $[\text{BuMeIm}][\text{Tf}_2\text{N}]$ and (\blacklozenge) $[\text{BuMe}_2\text{Im}][\text{Tf}_2\text{N}]$ or of a solution of $[\text{MeBu}_3\text{N}]_2[\text{UCl}_6]$ dissolved ($3 \times 10^{-3} \text{ M}$) in $[\text{BuMeIm}][\text{Tf}_2\text{N}]$ with addition of (\blacksquare) $[\text{MeBu}_3\text{N}][\text{Tf}_2\text{N}]$. $X = \text{BuMeIm}$ or BuMe_2Im .

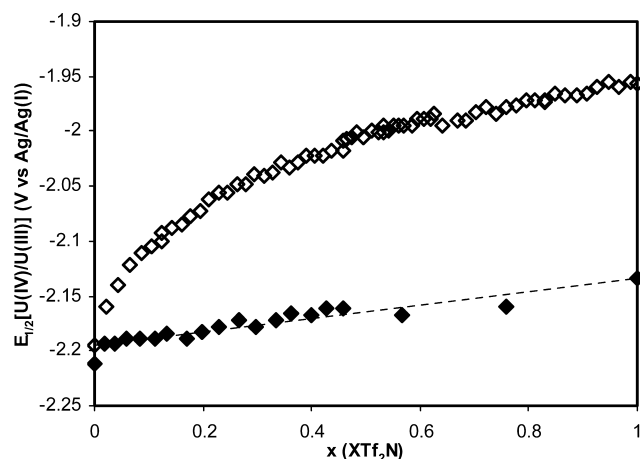


Figure 9. Half-wave potential of a solution of $[\text{MeBu}_3\text{N}]_2[\text{UCl}_6]$ dissolved ($3 \times 10^{-3} \text{ M}$) in $[\text{MeBu}_3\text{N}][\text{Tf}_2\text{N}]$ versus molar fraction of (\diamond) $[\text{BuMeIm}][\text{Tf}_2\text{N}]$ or (\blacklozenge) $[\text{BuMe}_2\text{Im}][\text{Tf}_2\text{N}]$ with a GC electrode (area 0.07 cm^2). $\nu = 100 \text{ mV s}^{-1}$; $X = \text{BuMeIm}$ or BuMe_2Im .

and $[\text{BuMeIm}][\text{Tf}_2\text{N}]$, respectively. The potential of the $\text{U}(\text{V})/\text{U}(\text{IV})$ couple is 0.18, 0.21, and 0.27 V vs $\text{Ag}/\text{Ag}(\text{I})$, respectively, in the same media.

Moreover, the higher intensity of the anodic and cathodic peak currents for the two redox couples observed in Figure 6 is attributable to an increase in the diffusion coefficient of the species. The viscosity of $[\text{MeBu}_3\text{N}][\text{Tf}_2\text{N}]$ is 362 cP ¹⁵ compared with only 93 cP for $[\text{BuMe}_2\text{Im}][\text{Tf}_2\text{N}]$ ²² and 52 cP for $[\text{BuMeIm}][\text{Tf}_2\text{N}]$.¹⁵ The high viscosity of $[\text{MeBu}_3\text{N}][\text{Tf}_2\text{N}]$ limits the diffusion of electroactive species compared with the other two ionic liquids, $[\text{BuMe}_2\text{Im}][\text{Tf}_2\text{N}]$ and $[\text{BuMeIm}][\text{Tf}_2\text{N}]$.

After characterization in pure ionic liquids, we carried out spectroscopic and electrochemical determinations by monitoring the absorbance and potential of the $\text{U}(\text{IV})/\text{U}(\text{III})$ couple while adding $[\text{BuMeIm}][\text{Tf}_2\text{N}]$ to a solution of $[\text{MeBu}_3\text{N}]_2[\text{UCl}_6]$ (0.01 M) in the ionic liquid $[\text{MeBu}_3\text{N}][\text{Tf}_2\text{N}]$. The same type of determination was carried out for $[\text{MeBu}_3\text{N}]_2[\text{UCl}_6]$ (0.01 M) in ionic liquid $[\text{MeBu}_3\text{N}][\text{Tf}_2\text{N}]$ by adding $[\text{BuMe}_2\text{Im}][\text{Tf}_2\text{N}]$.

Figure 7 shows the UCl_6^{2-} spectra after addition of $[BuMeIm][Tf_2N]$ and indicates a significant increase in the 597 nm peak. Figure 8 shows the variation in the absorbance ratio at 597 and 593.5 nm according to the $[BuMeIm][Tf_2N]$ molar fraction. The ratio increases as $[BuMeIm][Tf_2N]$ is added, reaching a value of 1.3, comparable to the value obtained after dissolving $[MeBu_3N]_2[UCl_6]$ directly in $[BuMeIm][Tf_2N]$.

The reverse determination was also carried out. Mass fractions of $[MeBu_3N][Tf_2N]$ were added to a solution of $[MeBu_3N]_2[UCl_6]$ dissolved in the ionic liquid $[BuMeIm][Tf_2N]$. The results are also indicated in Figure 8. The curve has the same shape as before. The change in the slope once again occurs for a $[BuMeIm][Tf_2N]$ concentration of about 1.4 mol L^{-1} , which corresponds to the addition of about 1.8 mol L^{-1} of $[MeBu_3N][Tf_2N]$. These results clearly demonstrate the reversibility of the interaction, confirming that equilibrium was reached between the anionic complex UCl_6^{2-} and the cation $BuMeIm^+$.

Figure 8 also shows the variation in the absorbance ratio at 597 and 593.5 nm versus the molar fraction of the added $[BuMe_2Im][Tf_2N]$. The variation remained constant as the ionic liquid was added, and the mean absorbance ratio was 1.03.

In the next step, the anodic and cathodic potentials of the U(IV)/U(III) couple were monitored electrochemically in $[MeBu_3N][Tf_2N]$ while $[BuMeIm][Tf_2N]$ was added. Figure 9 shows the variation in the half-wave potential of the U(IV)/U(III) couple versus the $[BuMeIm][Tf_2N]$ molar fraction. The potential increases as $[BuMeIm][Tf_2N]$ is added, reaching a constant value of -1.95 V vs Ag/Ag(I) corresponding to the value obtained in pure $[BuMeIm][Tf_2N]$. During titration, the potential of the U(IV)/U(III) couple shifted by 250 mV. Note that the potential of the ferrocene/ferricinium (Fc^+/Fc) couple is unchanged during the determination (Figure S8) and remains constant at -0.35 V vs Ag/Ag(I). The variation recorded during electrochemical determination of UCl_6^{2-} is indeed the result of an interaction between the ionic liquid cation and the redox species of the U(IV)/U(III) couple.

Figure 9 shows the potential variation for the U(IV)/U(III) couple of $[MeBu_3N]_2[UCl_6]$ dissolved in $[MeBu_3N][Tf_2N]$ versus the $[BuMe_2Im][Tf_2N]$ molar fraction. The potential of this couple increases slightly from -2.2 to -2.13 V versus Ag/Ag(I), values that correspond to the potentials of the U(IV)/U(III) couple of $[MeBu_3N]_2[UCl_6]$ in the ionic liquids $[MeBu_3N][Tf_2N]$ and $[BuMe_2Im][Tf_2N]$, respectively. The slight increase (70 mV) indicates competition between the two cations $MeBu_3N^+$ and $BuMe_2Im^+$ during solvation of these species.

The U(IV)/U(III) and U(V)/U(IV) redox couples are rapid and reversible.¹⁵ The species of these two redox couples include $U^{III}Cl_6^{3-}$, $U^{IV}Cl_6^{2-}$, and $U^VCl_6^-$. The more positive potential of the U(IV)/U(III) couple in $[BuMeIm][Tf_2N]$, if compared with $[MeBu_3N][Tf_2N]$, indicates stronger interaction between the anionic complex $U^{III}Cl_6^{3-}$ and $[BuMeIm][Tf_2N]$ than that in $[MeBu_3N][Tf_2N]$. Modeling studies performed recently by Schurhammer and Wipff confirm this observation.¹⁷ Conversely, the slight potential difference of

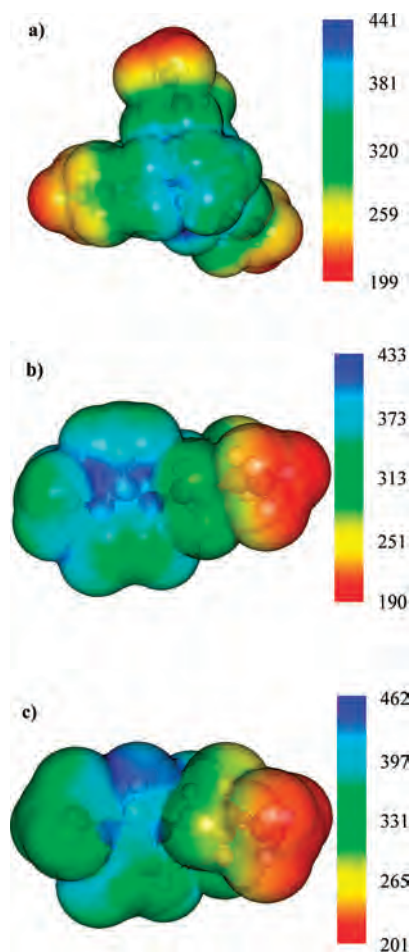


Figure 10. Electrostatic potential surface (kJ mol^{-1}) of cations (a) $MeBu_3N^+$, (b) $BuMe_2Im^+$, and (c) $BuMeIm^+$.

Table 9. Minimum Electrostatic Potential Energy of Ionic Liquid Anions and UCl_6^{2-}

anion	electrostatic potential energy (kJ mol^{-1})
Tf_2N^-	-446
PF_6^-	-488
Tf^-	-509
BF_4^-	-533
UCl_6^{2-}	-711

Table 10. Maximum Electrostatic Potential Energy for Each Ionic Liquid Cation

cation	electrostatic potential energy (kJ mol^{-1})
$BuMeIm^+$	468
$BuMe_2Im^+$	460
$MeBu_3N^+$	424

the U(V)/U(IV) couple can be attributed to a similar interaction with the medium containing the two species of the redox couple ($U^{IV}Cl_6^{2-}$ and $U^VCl_6^-$).

4. Discussion

During this study, we observed a hydrogen bonding between the ionic liquid cation ($BuMeIm^+$, $BuMe_2Im^+$ or $MeBu_3N^+$) and the anionic complex UCl_6^{2-} . The interaction is demonstrated by distortion of the octahedral complex UCl_6^{2-} . Absorption spectroscopy of the solutes in solid form or in solution reveals a band at 597 nm depending on the

ionic liquid cation used. This distortion allows the Laporte-forbidden $5f \rightarrow 5f$ transition to be observed for a centrosymmetric complex as proposed by Ryan.¹⁸ The modified potentials of the U(IV)/U(III) and U(V)/U(IV) redox couples observed depending on the ionic liquid also indicate an interaction between the cation and the UCl_6^{2-} complex as reported by Nikitenko et al.¹⁵ The distortion of the UCl_6^{2-} anionic complex is also shown by a change in the U–Cl distances obtained by EXAFS in solution and by single-crystal XRD for the solid compounds, although this distortion does not lead to destruction of the octahedral structure.

The experimental results obtained also show that the anionic complex UCl_6^{2-} exhibits different behavior depending on the ionic liquid cation. To identify the protons responsible for this interaction, we used the following ionic liquid cations: $MeBu_3N^+$, $BuMe_2Im^+$, and $BuMeIm^+$. Unlike $BuMeIm^+$, $BuMe_2Im^+$ features a methyl group on the C(2) atom replacing the most acidic proton.

The protons involved in this interaction were identified, notably by infrared spectroscopy: the change in the wavenumbers of the vibration bands indicates the chemical function responsible for the interaction. This result was corroborated by NMR measurements of the $BuMeIm^+$ cation. Anion/cation distances shorter than the Van der Waals radius of H and Cl atoms determined by single-crystal XRD also indicate the protons involved in this interaction. These results were validated by ab initio calculations. The location of the interaction on the various cations is characterized by a maximum electrostatic potential surface shown in blue in Figure 10.

The hydrogen bond was shown to be established between the chlorides of the anionic complex UCl_6^{2-} and the protons on the α -carbon atoms of nitrogen ($N-CH_3$ and $N-CH_2-$) for the $MeBu_3N^+$ cation, the protons of the methyl groups of the imidazolium ring for the $BuMe_2Im^+$ cation, and the most acidic proton on carbon 2 for the $BuMeIm^+$ cation.

The cation $BuMeIm^+$ thus interacts mainly with the anionic complex UCl_6^{2-} via most acidic proton on carbon 2 and not via the other protons, confirming the work by Nikitenko et al.²⁰

IR and NMR measurements also showed that the intensity of the association between $BuMeIm^+$ and the anions increases in the following order: $PF_6^- < BF_4^- < Tf_2N^- < Tf^- < Cl^- < UCl_6^{2-}$. Ab initio calculations also confirmed these results. Table 9 gives the minimum electrostatic potential energy values of these anions. The order of magnitude of the electrostatic potential energies for the two linear anions ($Tf^- > Tf_2N^-$) and for the spherical anions ($UCl_6^{2-} > BF_4^- > PF_6^-$) coincides with the redshift observed for the aromatic ring vibration bands and the unshielding of proton H(2) of the $BuMeIm^+$ cation. The weak unshielding observed by NMR and the slight IR wavenumber shift for the two spherical anions BF_4^- and PF_6^- are caused by the equal charge distribution on each fluorine atom which diminishes the cation interaction, as demonstrated by Tokuda et al.³² The higher intensity of the ionic association between the $BuMeIm^+$ cation and the UCl_6^{2-} anion probably arises from the -2 charge of the anionic complex.

UV–vis absorption spectroscopy and electrochemistry determinations show an increase in the absorbance peak at 597 nm and a variation of the potentials of the U(IV)/U(III) and U(V)/U(IV) redox couples, indicating a difference in the association between the ionic liquid cations and the anionic complex UCl_6^{2-} . The maximum electrostatic potential energy for the cations (Table 10) confirms these experimental results.

The intensity of the association between the UCl_6^{2-} anionic complex and the cations increases in the following order: $BuMeIm^+ \gg BuMe_2Im^+ \approx MeBu_3N^+$.

5. Conclusion

The three cations of ionic liquids $MeBu_3N^+$, $BuMe_2Im^+$, and $BuMeIm^+$ studied here demonstrate the existence of a hydrogen bonding between these cations and the UCl_6^{2-} anion in the solid and in solution.

The intensity of the interactions was evaluated by characterizing the two solids $[MeBu_3N]_2[UCl_6]$ and $[BuMe_2Im]_2[UCl_6]$ and by studying $[MeBu_3N]_2[UCl_6]$ in solution and in different ionic liquids: $[MeBu_3N][Tf_2N]$, $[BuMeIm][Tf_2N]$, and $[BuMe_2Im][Tf_2N]$. The UCl_6^{2-} anion interacts with the cations in the following order: $MeBu_3N^+ \approx BuMe_2Im^+ \ll BuMeIm^+$. The interaction between the anion and cation mainly involves the protons on the α -carbon atoms of nitrogen of $MeBu_3N^+$ and the protons of the methyl groups of the imidazolium ring for $BuMe_2Im^+$. The interaction previously observed for the $[BuMeIm]_2[UCl_6]$ complex²⁰ was confirmed and corresponds to a hydrogen bond between most acidic proton (C2) of the imidazolium ring and the chlorides of the UCl_6^{2-} anion.

Acknowledgment. The authors are grateful to CEA/DEN/DSOE/RB and ACTINET Network for financial support. XAS measurements were carried out at ESRF, a European user facility, and at Stanford Synchrotron Radiation Laboratory, a national user facility operated by Stanford University on behalf of the US department of Energy, Office of Basic Energy Sciences. The authors thank C. Hennig, A. Scheinost, H. Funke and A. Rossberg (ESRF/ROBL), J. Bargar and J. Rogers (SSRL/11-2), and S. D. Conradson (LANL) for their help. The authors are grateful to Sébastien Petit for assistance with RMN.

Supporting Information Available: IR spectra of solid $[MeBu_3N]_2[UCl_6]$, solid $[BuMeIm]_2[UCl_6]$, and solid $[BuMe_2Im]_2[UCl_6]$, visible absorption spectra of solid $[BuMe_2Im]_2[UCl_6]$ and solid $[MeBu_3N]_2[UCl_6]$, relation between chemical shifts of $[MeBu_3N]Cl$ and $[MeBu_3N]_2[UCl_6]$, experimental and fitted U L_{III}-edge k^3 of $[MeBu_3N]_2[UCl_6]$ dissolved (0.01 M) in $[MeBu_3N][Tf_2N]$ and $[BuMe_2Im]_2[UCl_6]$ dissolved (0.01 M) in $[BuMe_2Im][Tf_2N]$, UV–vis spectra of $[BuMeIm]_2[UCl_6]$, $[BuMe_2Im]_2[UCl_6]$, and $[MeBu_3N]_2[UCl_6]$ dissolved ($7.74 \times 10^{-3}M$), respectively, in $[BuMeIm][Tf_2N]$, $[BuMe_2Im][Tf_2N]$, and $[MeBu_3N][Tf_2N]$, half-wave potential of a ferrocene solution dissolved (0.01 M) in $[MeBu_3N][Tf_2N]$

(32) Tokuda, H.; Tsuzuki, S.; Abu Bin Hasan Susan, M.; Hayamizu, K.; Watanabe, M. *J. Phys. Chem. B* **2006**, *110*, 19593–19600.

Solvation of UCl_6^{2-} Anionic Complex

versus molar fraction of [BuMeIm][Tf₂N] with a GC electrode (area 0.07 cm²) at 25 °C. $v = 100$ mV s⁻¹, and electrostatic potential charges used to simulate different ions of ionic liquids.

This material is available free of charge via the Internet at <http://pubs.acs.org>.

IC702477Z